MOLECULAR AND CELLULAR BIOLOGY, May 2003, p. 3202–3215 Vol. 23, No. 9
0270-7306/03/$08.00+0 DOI: 10.1128/MCB.23.9.3202–3215.2003

The Yeast RSC Chromatin-Remodeling Complex Is Required for Kinetochore Function in Chromosome Segregation

Jing-mei Hsu,[1] Jian Huang,[1] Pamela B. Meluh,[2] and Brehon C. Laurent[1]*

Department of Microbiology and Immunology, Morse Institute of Molecular Biology and Genetics, and Program in Molecular and Cellular Biology, State University of New York, Brooklyn, New York 11203,[1] and Molecular Biology Program, Memorial Sloan-Kettering Cancer Center, New York, New York 10021[2]

Received 13 January 2003/Accepted 4 February 2003

The accurate segregation of chromosomes requires the kinetochore, a complex protein machine that assembles onto centromeric DNA to mediate attachment of replicated sister chromatids to the mitotic spindle apparatus. This study reveals an important role for the yeast RSC ATP-dependent chromatin-remodeling complex at the kinetochore in chromosome transmission. Mutations in genes encoding two core subunits of RSC, the ATPase Sth1p and the Snf5p homolog Sfh1p, interact genetically with mutations in genes encoding kinetochore proteins and with a mutation in centromeric DNA. RSC also interacts genetically and physically with the histone and histone variant components of centromeric chromatin. Importantly, RSC is localized to centromeric and centromere-proximal chromosomal regions, and its association with these loci is dependent on Sth1p. Both *sth1* and *sfh1* mutants exhibit altered centromeric and centromere-proximal chromatin structure and increased missegregation of authentic chromosomes. Finally, RSC is not required for centromeric deposition of the histone H3 variant Cse4p, suggesting that RSC plays a role in reconfiguring centromeric and flanking nucleosomes following Cse4p recruitment for proper chromosome transmission.

The segregation of sister chromatids during cell division ensures that each daughter cell receives a complete copy of the genome. The accuracy of chromosome transmission depends on the coordination of events in the chromosome cycle. Sister chromatid cohesion is first established during DNA replication or shortly thereafter and is maintained as chromosomes condense and align themselves on the mitotic spindle until the onset of anaphase. The attachment of chromosomes to the mitotic spindle is mediated by kinetochores, multiprotein complexes that assemble onto centromeric DNA. When all sister chromatids achieve bipolar kinetochore-microtubule orientation, cohesion is dissolved, and sister chromatids segregate to opposite spindle poles (70). Defects in any of these steps can result in aneuploidy, which can lead to unregulated cell growth or death. Cellular surveillance pathways such as the spindle checkpoint closely monitor kinetochore-microtubule interactions to ensure that chromosome alignment, orientation, and segregation occur with fidelity (1, 62).

Centromere function in the budding yeast *Saccharomyces cerevisiae* is conferred by an unusually compact 125-bp DNA sequence comprised of three conserved elements, CDEI, CDEII, and CDEIII, which are necessary and sufficient to mediate segregation of sister chromatids (12, 29). CDEI and CDEIII are highly conserved palindromic sequences that flank the nonconserved AT-rich CDEII sequence (29). This comparatively simple point yeast centromere is nevertheless capable of assembling a complex kinetochore structure resembling that of higher eukaryotes. Binding of the CBF3 complex to CDEIII is thought to nucleate kinetochore assembly, thereby playing a central role in kinetochore function (32, 41). Binding of the Cbf1p dimer to CDEI induces DNA bending in a manner thought to be important for stabilization of higher-order kinetochore structure (32). In addition to Cbf1p and the CBF3 complex, the centromere-specific histone H3 variant Cse4p, a homologue of the human CENP-A protein, and Mif2p, a homologue of human CENP-C, also interact with centromeric DNA elements (41, 43, 48). The attachment of the kinetochore to spindle microtubules requires outer kinetochore protein complexes. Central kinetochore complexes, such as CTF19, link these outer microtubule-binding complexes to the inner kinetochore (14).

Several studies in the budding yeast *S. cerevisiae* suggest that chromatin structure is critical for centromere-kinetochore function and chromosome segregation (56, 68). Centromeric chromatin of *S. cerevisiae* consists of a 160- to 220-bp nuclease-resistant domain demarcated by strong nuclease-hypersensitive sites flanked by highly ordered pericentromeric chromatin (56). The core centromeric chromatin is marked by the presence of the histone H3 variant Cse4p. These specialized H3 histones are present at active centromeres in all eukaryotes examined, from *S. cerevisiae* to humans (68). Specific mutations in the genes encoding histones H2A, H2B, and H4 and the histone H3 variant as well as in the CDE elements alter the nuclease digestion patterns of both core centromeric and centromere-proximal regions and have been shown to impair mitotic chromosome segregation in *S. cerevisiae* (25, 43, 51, 54, 55). Genetic evidence from *S. cerevisiae* suggests that centromeric chromatin includes a histone octamer in which the histone H3 variant replaces histone H3 (63, 68). How this specialized nucleosome is assembled and targeted to the centromere and how it contributes to kinetochore assembly are largely unknown.

Eukaryotic chromatin undergoes dynamic structural changes throughout the cell division cycle. These structural alterations range from the local changes necessary for transcriptional regulation to global changes necessary for chromosome segregation. Several evolutionarily conserved protein complexes

* Corresponding author. Mailing address: Department of Microbiology & Immunology, SUNY Downstate Medical Center, 450 Clarkson Ave., Box 44, Brooklyn, NY 11203. Phone: (718) 270-3755. Fax: (718) 270-2656. E-mail: brehon.laurent@downstate.edu.

capable of modifying histones or altering histone-DNA interactions have been identified. These chromatin-modifying complexes can be grouped into two major classes. The first class of enzymes covalently modifies histones and includes histone acetyltransferases, kinases, histone deacetylases, and histone methyltransferases (66). The second class of remodelers, represented by the SWI/SNF and related ISWI, CHD, Mi-2/NURD, and Ino80 families, has a common subunit in the Snf2p/Swi2p family of ATPases and uses the energy of ATP hydrolysis to disrupt histone-DNA interactions (4, 59, 76). Several of these ATP-dependent remodelers can function in conjunction with histone-modifying complexes to regulate access of transcription factors to nucleosomal DNA (35, 67). Roles for chromatin remodelers in DNA replication, DNA repair, and recombination have also been reported (20). RSC (for remodels the structure of chromatin) is a 15-protein ATP-dependent remodeling complex in the SWI/SNF family that is essential for viability and cell cycle progression (2, 10, 11, 17, 37, 74). Four of the RSC proteins, Sth1p, Sfh1p, Rsc8p, and Rsc6p, are highly similar to the SWI-SNF subunits Snf2p, Snf5p, Swi3p, and Swp73p, respectively. Genetic analysis and genome-wide localization and expression studies suggest roles for RSC in the cellular response to stress, nitrogen and carbohydrate metabolism, mitochondrial function, and the regulation of RNA polymerase III-mediated transcription (2, 13, 15, 17, 45, 47).

Previously, two studies implicated RSC in chromosome and plasmid transmission (73, 77). Here, we report a role for RSC at kinetochores in chromosome segregation. RSC interacts genetically and physically with kinetochore components and is localized to centromeric and centromere-proximal regions. Centromeric chromatin structure is altered in *sth1-3ts* and *sfh1-1ts* mutants, and RSC localization is impaired in *sth1-3ts* mutants. Moreover, sister chromatids are missegregated in both *rsc* mutants. Interestingly, RSC appears to be dispensable for the centromeric deposition of the kinetochore proteins Cse4p and Mif2p. We propose that the RSC nucleosome remodeler is required for configuring centromeric and flanking chromatin structure that supports proper kinetochore function.

MATERIALS AND METHODS

Strains, plasmids, and genetic methods. The *S. cerevisiae* strains used had either the S288c or W303 genetic background and are listed in Table 1. Plasmids used in this study are listed in Table 2. Strain constructions and genetic manipulations were carried out by standard methods (53). All yeast media were prepared as described previously (53). Yeast cultures were grown in rich medium, consisting of yeast extract, peptone, and 2% dextrose (YPD), or selective synthetic complete (SC) medium containing 2% dextrose. Adenine indicator plates for the chromosome segregation assay contained synthetic complete minimal medium supplemented with adenine (6 μg/ml) to enhance coloration. For synchronization of cells in G_1 phase, α-factor was added to a final concentration of 15 μg/ml; for S phase, hydroxyurea was added to a final concentration of 0.1 M; and for G_2/M phase, nocodazole was added to a final concentration of 15 μg/ml. Temperature shift experiments and fluorescence-activated cell sorting analysis were performed as described previously (11, 17). To determine viability, cells grown at the nonpermissive temperature were briefly sonicated and plated onto YPD medium at a concentration of ≈250 cells/plate at the indicated times.

Diploid strain BLY297 (*swh3*Δ::*HIS3*/*SWH3 ura3*/*ura3*) was transformed with pJMH2 or pJMH1 to uracil prototrophy, and the transformants were sporulated and subjected to tetrad dissection. The recovered *swh3*Δ spore clones carrying pJMH2 or pJMH1 were named strains BLY298 and BLY301, respectively. Strains BLY295 (*mad1*Δ) and BLY296 (*sfh1-1ts mad1*Δ) were constructed by one-step gene disruption with the *Sma*I-*Sal*I fragment of pUC*mad1*Δ::*TRP1* (73). pJMH2 was created by cloning the *Eco*RI-*Sal*I fragment of pIT340 (71) into pRS316 (61). pJMH1 differs from pJMH2 in that the hemagglutinin (HA) tag was removed by *Not*I digestion.

Chromosome segregation assay. Chromosome missegregation events were analyzed by a visual colony color-sectoring assay, and the rate of artificial chromosome fragment loss was quantified as described previously (30, 36). Mid-logarithmic-phase homozygous wild-type and *sth1-3ts* cells were briefly sonicated and plated onto adenine indicator plates. The first cell cycle chromosome missegregation events were scored by counting red and white half-sectored colonies for chromosome nondisjunction (2:0) and by counting pink and red half-sectored colonies for chromosome loss events (1:0).

Far-Western assays. Histones were prepared by acid extraction, separated by sodium dodecyl sulfate (SDS)-polyacrylamide gel electrophoresis (PAGE), and blotted to polyvinylidene difluoride membranes as described previously (18). Radiolabeled Sth1p was prepared by translating Sth1p (pDJ91) in vitro in the presence of [^{35}S]methionine in a TNT-coupled reticulocyte lysate system (Promega) (11). Blots were hybridized and washed as described previously (18), and exposed to PhosphorImager screens.

GST pulldown assays. Glutathione *S*-transferase (GST) (pGEX-3X) or GST-histone fusion proteins (expressed from plasmids p307.3, p272.1, p284.1, p107.1, p289.6, and p184.1 in *Escherichia coli*) were prepared and bound to glutathione-Sepharose 4B resin equilibrated in binding buffer (20 mM HEPES [pH 7.5], 50 mM KCl, 2 mM $MgCl_2$, 0.5 mM EDTA, 0.5% [vol/vol] NP-40, 20% glycerol, 1 mM dithiothreitol, 1 mM phenylmethylsulfonyl fluoride). Five microliters of the reticulocyte lysate reaction mixture containing labeled Sth1p (as described previously for Far-Western assays) were incubated in binding buffer (with 50 μg of ethidium bromide per ml) with GST or GST-histone-Sepharose beads for 30 min at 25°C and then for 60 min at 4°C. Input levels of GST fusion proteins were normalized by Coomassie blue staining. The beads were then washed three times in binding buffer and resuspended in 1× SDS loading dye.

Immunoprecipitation. Extracts prepared from strains BLY309, BLY283, BLY573, BLY575, BLY572, and BLY574 expressing Flag-tagged histone H2B, H3, or H4 or control strains expressing untagged histones or containing empty vectors grown in YPD or SC medium selective for the plasmids were used to analyze coimmunoprecipitation of Sth1p with Flag-tagged histones. Extracts were prepared from cells grown to mid-logarithmic phase, and immunoprecipitation carried out in immunoprecipitation buffer (50 mM Tris [pH 7.4], 150 mM NaCl, 0.5% NP-40, 0.5 mg of bovine serum albumin per ml) in the presence of 250 U of DNase I for 2 h at 4°C as described previously (52). For each immunoprecipitation, 30 μl of anti-Flag M2 affinity resin (Sigma) was incubated with 2.5 mg of protein. Proteins released by boiling in SDS sample buffer were separated on an SDS–4 to 20% acrylamide gradient or 15% acrylamide gels and transferred to nitrocellulose for immunoblot analysis with a 1:1,000 dilution of polyclonal anti-Sth1p or a 1:300 dilution of anti-Flag M2 monoclonal antibody.

Chromatin immunoprecipitation. In vivo cross-linking and chromatin immunoprecipitation were performed as described previously (21) except that the lysis buffer contained 25 mM Tris-Cl [pH 8.0], 1 mM EDTA, 150 mM NaCl, 1 mM dithiothreitol, 1% Triton X-100, and 0.1% deoxycholate. The lysis and immunoprecipitation buffers used for chromatin immunoprecipitations in Fig. 7 were described previously (41). Sheared chromatin was immunoprecipitated with mouse monoclonal 12CA5 anti-HA (1:1,000), control monoclonal immunoglobulin G2b (the same isotype as the anti-HA antibody) (Roche Molecular Biochemicals), or polyclonal anti-Mif2p (1:250) (41) antibodies. PCR analysis of total and immunoprecipitated chromatin was carried out with primers to amplify target loci. Primer sequences are available upon request. Images were captured with a Bio-Rad Chemi Doc gel documentation system and analyzed with Quantity One quantitation software.

Chromatin structure analysis. *S. cerevisiae* nucleus preparation, micrococcal nuclease (MNase) digestion, and indirect end-labeling analysis of *CEN3* chromatin were performed as described previously (21, 51). DNA purified from MNase-treated nuclei was further digested with *Bam*HI, fractionated by agarose gel electrophoresis, and transferred to nitrocellulose membranes. *CEN3* DNA 5′ to CDEI was detected with the *CEN3* probe as described previously (51). The *Dra*I enzymatic accessibility assay and subsequent Southern blot analysis were performed as described previously (55). DNA was digested with *Hin*dIII following purification from *Dra*I-digested chromatin. The 0.9-kb *Bam*HI-*Hin*dIII fragment flanking CDEIII was labeled by random priming and used as a probe.

Microscopy. Strains carrying TetR-GFP (green fluorescent protein) were generated by transforming cells with the *Eco*RV-linearized plasmid pK3524 to direct integration at *LEU2*. To introduce TetO (TetR-arrays, approximately 228 bp 3′ of CDEIII of chromosome I and 35 kb from the *CEN* DNA of chromosome V, TetR-GFP-expressing wild-type and *rsc* mutant cells were transformed with the *Eco*RI fragment of pPM290 and the *Eco*RV-linearized pRS306-tetO(224) plas-

TABLE 1. *S. cerevisiae* strains

Strain[a]	Relevant genotype
BLY2	*MAT***a** *his3-Δ200 ura3-52 ade2-101 leu2-3,112 trp1-901 URA3::lexAop-lacZ gal4 gal80*
BLY46	*MAT***a** *his3-11,15 ura3-1 ade2-1 leu2-3,112 trp1-1 can1-100*
BLY49	*MAT***a** *sth1-3ts his3-Δ200 ura3-52 ade2-101*
BLY75-1	*MATα sfh1-1::HIS3 his3-11,15 ura3-1 ade2-1 leu2-3,112 trp1-1 can1-100*
BLY76	*MAT***a** *his3-Δ200 ura3-52 ade2-101 lys2-801*
BLY278	*MAT***a** *ura3-52 lys2-801 ade2-101 trp1-Δ1 his3-Δ200 leu2-Δ1*
BLY283	*MAT***a** *htb1-1 htb2-2 ura3-1 his3-11,15 ade2-1 leu2-3,112 trp1-1 can1-100* (pRS314-HTB1)
BLY295	*MAT***a** *mad1Δ::TRP1 his3-11,15 ura3-1 ade2-1 leu2-3,112 trp1-1 can1-100*
BLY296	*MAT***a** *sfh1-1::HIS3 mad1Δ::TRP1 his3-11,15 ura3-1 ade2-1 leu2-3,112 trp1-1 can1-100*
BLY298	*MAT***a** *swh3Δ::HIS3 his3-Δ200 ura3-52 lys2-801* pJMH2 (*CEN URA3 SWH3-HA*)
BLY301	*MAT***a** *swh3Δ::HIS3 his3-Δ200 ura3-52 lys2-801 leu2-3,112* pJMH1 (*CEN URA3 SWH3*)
BLY309	*MAT***a** *htb1-1 htb2-2 ura3-1 his3-11,15 ade2-1 leu2-3,112 trp1-1 can1-100* (pRS314-Flag-HTB1)
BLY353	*MAT***a** *sfh1-1::HIS3 his3-Δ200 ura3-52 ade2-101 lys2-801 leu2-Δ1 trp1-Δ1*
BLY360	*MATα sth1-3ts his3-Δ200 ura3-52 ade2-101 leu2-Δ1 lys2-801 CFIII (CEN3L.YPH278) URA3 SUP11*
BLY361	*MATα STH1 his3-Δ200 ura3-52 ade2-101 leu2-Δ1 lys2-801 CFIII (CEN3L.YPH278) URA3 SUP11*
BLY363	*MAT***a**/*MATα his3-Δ200/his3-Δ200 ura3-52/ura3-52 leu2-Δ1/LEU2 lys2-801/lys2-801 ade2-101/ade2-101* CFIII (*CEN3L.YPH278*) *URA3 SUP11*
BLY394	*MAT***a**/*MATα sth1-3ts/sth1-3ts his3-Δ200/his3-Δ200 ura3-52/ura3-52 ade2-101/ade2-101 leu2-Δ1/LEU2 lys2-801/LYS2* CFIII (*CEN3L.YPH278*) *URA3 SUP11*
BLY397	*MAT***a** *MCD1-6HA ura3 leu2*
BLY398	*MAT***a** *MCD1 ura3 leu2*
BLY413	*MAT***a** *ura3-52 leu2-3,112 lys2Δ200 HHT hhf1-20 Δ(HHT1-HHF1) Δ(HHT2-HHF2)*
BLY415	*MATα ura3-52 lys2 his3-Δ200 HHT hhf1-20 Δ(HHT1-HHF1) Δ(HHT2-HHF2)*
BLY416	*MATα mif2-3 his3-Δ200 ura3*
BLY424	*MAT***a** *ura3-52 ade2-101 trp1-Δ1 lys2-801 his3-Δ200 leu2-Δ1* CFIII(*D8B.d*) CDEII(+45) *URA3 SUP11 CEN6*
BLY429	*MAT***a** *ura3-52 ade2-101 trp1-Δ1 lys2-801 CFIII*(*D8B.d*) CDEI(8-C) *URA3 SUP11 CEN6*
BLY493	*MAT***a** *sth1-3ts his3-11,15 ade2-1 can1-100 leu2-3,112::GFP::tetR-LEU2 trp1-1 ura3-1::tetO-URA3*
BLY500	*MATα cse4-1 his3 ura3-52 ade2-101 lys2-801*
BLY503	*MATα ctf14-42 his3-Δ200 ura3-52 ade2 leu2-Δ1 lys2-801*
BLY506	*MAT***a** *ndc10-1 his3-Δ200 ura3 ade2 leu2 lys2 trp1 hom3? bar1:KAM?*
BLY520	*MAT***a** *his3-11,15 ade2-1 can1-100 leu2-3,112::GFP::tetR-LEU2 trp1-1 ura3-1 cen1::URA3-CEN3-tetO*
BLY526	*MATα sth1-3ts his3-11,15 ade2-1 can1-100 leu2-3,112::GFP::tetR-LEU2 trp1-1 ura3-1 cen1::URA3-CEN3-tetO*
BLY528	*MATα sth1-3ts ctf14-42 ura3-52 leu2-Δ1 his3-Δ200 lys2-801 ade2-101?*
BLY531	*MATα sth1-3ts mif2-3 ura3 his3-Δ200*
BLY532	*MATα sth1-3ts ndc10-1 his3-Δ200 ura3 ade2-101 hom3? bar1:KAM?*
BLY536	*MATα sth1-3ts cse4-1 his3 ura3-52 ade2-101 lys2-801*
BLY538	*MATα sfh1-1::HIS3 ndc10-1 his3-Δ200 ura3 ade2 leu2 lys2 trp1 hom3? barl:KAM?*
BLY546	*MATα sth1-3ts ura3-52 ade2-101 his3-Δ200 HHT hhf1-20* Δ(*HHT1-HHF1*) Δ(*HHT2-HHF2*)
BLY549	*MATα sth1-3ts swh3Δ::HIS3 ura3-52 his3-Δ200 ade2-101* pJMH2 (pRS316-HA-SWH3)
BLY552	*MAT***a** *sfh1-1::HIS3 lys2 ura3-52 trp1-*Δ200 *HHT hhf1-20* Δ(*HHT1-HHF1*) Δ(*HHT2-HHF2*)
BLY565	*MAT***a** *sth1-3ts ura3-52 ade2-101 lys2-801 his3-Δ200* CFIII(*D8B.d*) CDEI(8-C) *URA3 SUP11 CEN6*
BLY566	*MATα sth1-3ts ura3-52 ade2-101 leu2-Δ1 lys2-801 his3-Δ200* CFIII(*D8B.d*) CDEII(+45) *URA3 SUP11 CEN6*
BLY568	*MAT***a** *sth1-3ts his3-11,15 ura3-1::GFP-TUB1-URA3 ade2-1 leu2-3, 112 trp1-1 can1-100*
BLY570	*MAT***a** *his3-11,15 ura3-1::GFP-TUB1-URA3 ade2-1 leu2-3,112 trp1-1 can1-100*
BLY572	*MAT***a** *ura3-52 lys2-801 ade2-101 trp1-Δ1 his3-Δ200 leu2-Δ1* pRS315
BLY573	*MAT***a** *ura3-52 lys2-801 ade2-101 trp1-Δ1 his3-Δ200 leu2-Δ1* (Flag-H31) (pR5315)
BLY574	*MAT***a** *ura3-52 lys2-801 ade2-101 trp1-Δ1 his3-Δ200 leu2Δ1*(pRS424)
BLY575	*MAT***a** *ura3-52 lys2-801 ade2-101 trp1-Δ1 his3-Δ200 leu2-Δ1* (Flag-H4)
PM1311	*MAT***a** *ura3-52 ade2-101 his3-Δ200 lys2-801 STH1 CSE4-HA::URA3*
PM1312	*MAT***a** *ura3-52 ade2-101 his3-Δ200 LYS2 sth1-3ts CSE4-3HA::URA3*

[a] BLY2 is the same as CTY10-5d (obtained from R. Sternglanz); BLY278 and BLY424 are the same as YPH250 and YPH433 respectively (obtained from P. Hieter); BLY397 and BLY398 are the same as 1377A1-4B and 983-8A, respectively (obtained from P. Megee and D. Koshland); and BLY413 is the same as MSY554 (obtained from M. M. Smith).

mid (44), respectively. Correct integrations were verified by Southern blot analysis. Strains carrying *GFP-TUB1* were generated by transformation with the *Stu*I-linearized plasmid pAFS125. To visualize TetR-GFP-marked chromosomal loci or GFP-marked tubulin, paraformaldehyde-fixed cells were imaged on a Nikon Microphot 2 microscope with a 100×, 1.4 NA oil immersion lens. Images were acquired with a Spot-RT charge-coupled device-cooled camera with SPOT diagnostic software.

RESULTS

***rsc* mutants activate the spindle checkpoint and missegregate chromosomes.** Mutations in the essential genes encoding the core RSC Sth1p ATPase and Sfh1p subunits *sth1-3ts*, *nps1-105* (a different *sth1* allele), and *sfh1-1ts* were previously shown to cause conditional cell cycle arrest at G_2/M, suggesting that RSC function is required for cell cycle progression (11, 17, 73). Initial analysis of several classes of genes encoding proteins required for mitotic cell division, including cyclins (*CLN3*, *CLB2*), kinetochore components (*CSE4*, *NDC10*), and the mitotic segregation apparatus (*TUB1*, *TUB3*) revealed no obvious defects in the transcription of these genes in the *sth1-3ts* or *sfh1-1ts* mutant (13, 17; J.-M. Hsu and B. C. Laurent, unpublished data). We tested whether the preanaphase checkpoints that respond to damaged DNA or defective kinetochore-mi-

TABLE 2. Plasmids

Plasmid	Description[a]	Source or reference
pJMH1	pRS316-SWH3 (*CEN6, URA3*)	This study
pJMH2	pRS316-HA-SWH3 (*CEN6, URA3*)	This study
YEp24	2μm, *URA3*, Amp^r	31
pYC5H	*SFH1* in YEp24 (2μm, *URA3*)	11
pPY3	*CSE4* (2μm, *URA3*)	22
pPM47	*NDC10, 2μm, URA3*	42
pPM290	~11.2-kb *Kpn*I fragment from pRS306-tetOp(224) subcloned into pUC19-based *CEN1* replacement vector pPM101	42
pACT2	*GAD*, 2μm, *LEU2*	38
pJL484	*GAD-CSE4*, 2μm, *LEU2*	48
pJL486	*GAD-MIF2*, 2μm, *LEU2*	48
pJO196	*GAD-NDC10*, 2μm, *LEU2*	48
pGAD-CTF19	*GAD-CTF19*, 2μm, *LEU2*	48
pSH2-1	2μm, *HIS3*	26
pLexA$_{202}$-Sth1$_{1-1359}$	2μm, *HIS3*	11
pIT331	*GAD-SWH3/RSC8*, 2μm, *LEU2*	72
pDJ91	*STH1*, 2μm, *URA3*	11
pK3524	NLS-*tetR-GFP* LEU2	44
pRS306-tetO(224)	*URA3*	44
pAFS125	pTUB1-GFP	A. W. Murray
p307.3	pGEX-2T (histone H3 residues 21–46)	28
p272.1	pGEX-2T (histone H4 15–34)	28
p284.1	pGEX-2T (histone H4 1–16)	28
p107.1	pGEX-2T (histone H4 1–34)	28
p289.6	pGEX-2T (histone H3 1–25)	28
p184.1	pGEX-2T (histone H3 1–46)	28
pFlag-H4	1.9-kb *Eco*RI-*Bam*HI fragment of 2μm-*URA3* Flag-H4 (gift of M. A. Osley) cloned into pRS424	
pFlag-H3	2.0-kb *Xho*I-*Bam*HI fragment of pPM416 (pRS314-Flag-H3) into pRS315	
pRS424	2μm, *TRP1*	60
pRS315	*CEN6/ARSH4*	60

[a] NLS, nuclear localization signal.

crotubule interactions were activated in these mutants. We found that two key components of the DNA damage checkpoint, *RAD9* and *MEC1*, were not required for arrest of *sth1-3ts* or *sfh1-1ts* cells (17; I. Nasir and B. C. Laurent, unpublished). In contrast, both the *sth1-3ts* and *sfh1-1ts* mutations activated the *MAD1* spindle checkpoint (Fig. 1A; only *sfh1-1ts* is shown). Flow cytometry analysis of DNA content revealed that inactivation of the spindle checkpoint by the *mad1*Δ mutation permitted a significant percentage of the *sfh1-1ts mad1*Δ cells to complete mitosis (Fig. 1A, upper panel). Furthermore, fewer than 7% of the *sfh1-1ts mad1*Δ double mutants were viable, while the corresponding single-mutant viability remained high 8 h following a shift to 37°C (Fig. 1A, lower panel), indicating that the spindle checkpoint is required to arrest *sfh1-1ts* at G_2/M and to maintain its viability. These results are in agreement with previous results showing that *nps1-105*, a different allele of *sth1*, and *rsc3-3* similarly engaged the *MAD1*-dependent checkpoint to arrest cells in G_2/M (2, 73).

Activation of the spindle checkpoint by the *rsc* mutations indicates a potential role for RSC in centromere-kinetochore function, as this checkpoint monitors the integrity of kinetochores and microtubules, kinetochore-microtubule interactions, and the tension resulting from bipolar attachment (1, 14). Consistent with this idea, we found that both *sth1-3ts* and *sfh1-1ts* mutants were sensitive to the microtubule-depolymerizing agents benomyl and thiabendazole (TBZ), which perturb the chromosome segregation machinery (data not shown; see also Fig. 2B) (13). We also found that the homozygous *sth1-3ts* diploids missegregated a linear reporter chromosome fragment by using a colony color-sectoring assay. The *sth1-3ts* mutants exhibited sixfold higher rates of 2:0 chromosome nondisjunction than isogenic wild-type strains (6.1×10^{-3} versus

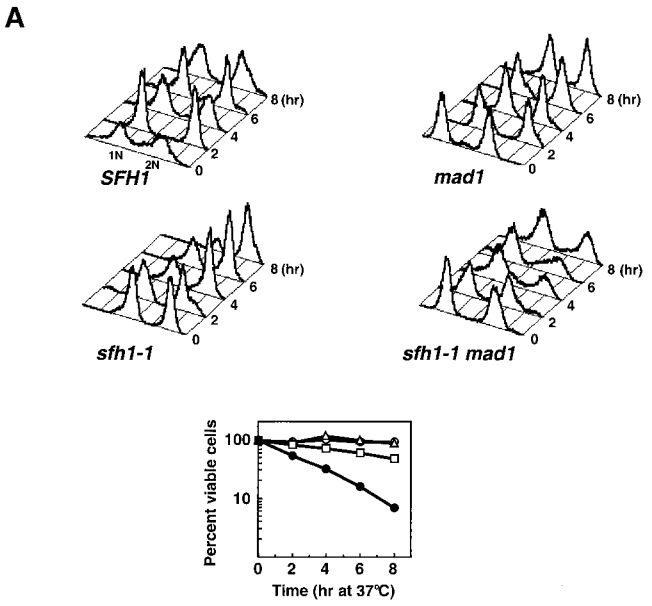

B

		2:0 event (R/W)	1:0 event (R/P)	Total
STH1/*STH1*	25°C	0	1.4×10^{-3}	4493
	37°C → 25°C	1.1×10^{-3}	0.9×10^{-3}	5994
sth1-3ts/*sth1-3ts*	25°C	0	1.4×10^{-3}	4622
	37°C → 25°C	6.1×10^{-3}	1.3×10^{-3}	6027

FIG. 1. *rsc* mutants exhibit phenotypes characteristic of mutants defective in chromosome segregation. (A) *sfh1-1ts* activates the *MAD1*-dependent spindle checkpoint pathway. Upper panel: Flow cytometric analysis of DNA contents in *SFH1* (BLY46), *mad1* (BLY295), *sfh1-1ts* (BLY75-1), and *sfh1-1ts mad1* (BLY296) strains at the times indicated. Cells grown to mid-logarithmic phase at 25°C were shifted to 37°C, and aliquots were removed for analysis at the times indicated. The number of cells was plotted versus the relative intensity of emitted light. Lower panel: At the times indicated, the *SFH1* (open circles), *mad1* (open triangles), *sfh1-1ts* (open squares), and *sfh1-1ts mad1* (solid circles) cells described above were removed from 37°C and plated onto YPD medium at 25°C. Viability was determined as the number of cells capable of forming colonies at 25°C. Values reported are the averages for two independent determinations with <15% error. (B) Homozygous *sth1-3ts* diploid cells exhibit increased 2:0 missegregation of a chromosome fragment. *STH1*/*STH1* (BLY363) and *sth1-3ts*/*sth1-3ts* (BLY394) cells carrying a single copy of CFIII were incubated at 37°C for 4 h before shifting back to 25°C. Red sectors indicate loss of chromosomes, and white sectors indicate gain of chromosomes. Half-sectored colonies were scored as R/W (half red/half white) or R/P (half red/half pink) after 2 to 4 days of incubation. The rates of CFIII nondisjunction (2:0 segregation) and loss (1:0 segregation) were calculated by dividing the number of half red/half white and half red/half pink cells, respectively, by the total number of pink parental cells indicated. The data from two independent experiments were combined.

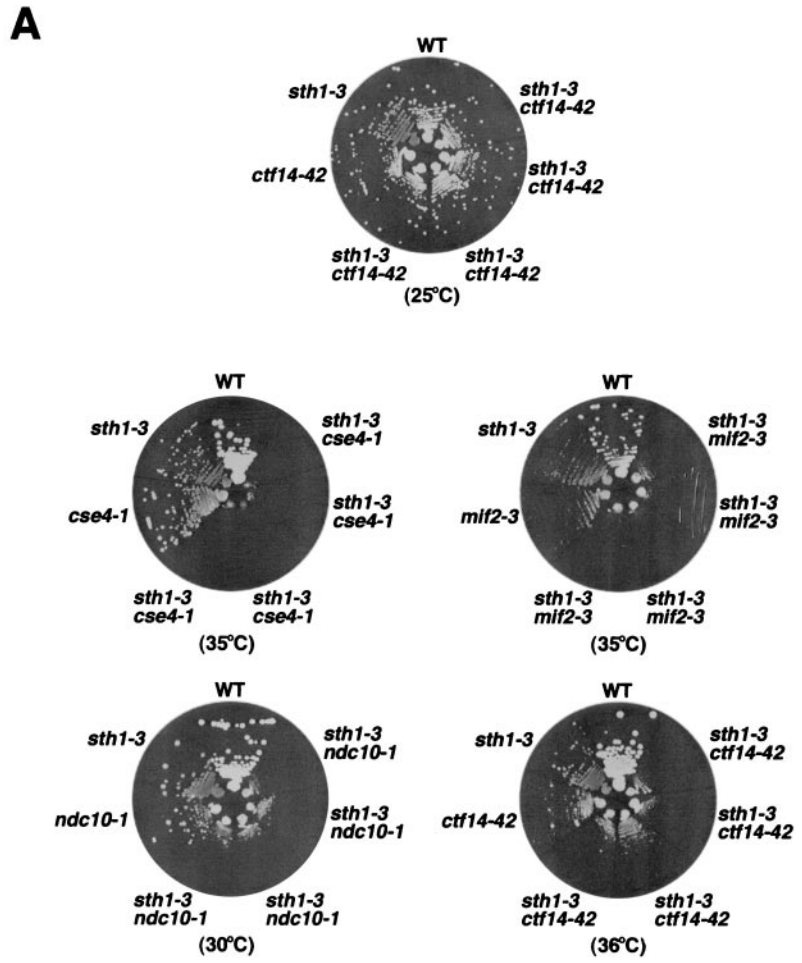

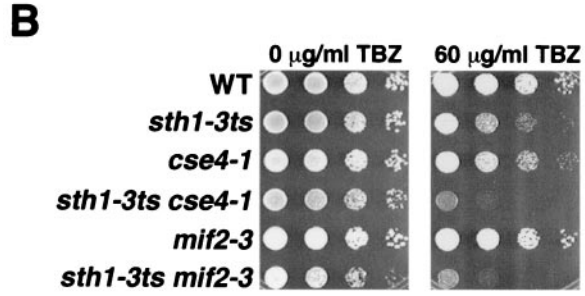

FIG. 2. RSC interacts genetically with components of the kinetochore. (A) *sth1-3ts* interacts with mutations in kinetochore components. The genotypes refer to the following strains: wild type (WT, BLY76), *sth1-3* (BLY49), *ctf14-42* (BLY503), *sth1-3 ctf14-42* (BLY528), *cse4-1* (BLY500), *sth1-3 cse4-1* (BLY536), *mif2-3* (BLY416), *sth1-3 mif2-3* (BLY531), *ndc10-1* (BLY506), and *sth1-3 ndc10-1* (BLY532). Strains were grown on YPD plates at the indicated temperatures for 3 to 4 days. Four independently isolated double mutant strains were tested on each plate. (B) *sth1-3ts* mutations in combination with either *cse4-1* or *mif2-3* mutations cause enhanced hypersensitivity to TBZ. Tenfold serial dilutions of mid-logarithmic-phase cells were spotted onto YPD plates containing 0 or 60 μg of TBZ per ml. Growth of wild-type (BLY76), *sth1-3ts* (BLY49), *cse4-1* (BLY500), *sth1-3ts cse4-1* (BLY536), *mif2-3* (BLY416), and *sth1-3ts mif2-3* (BLY531) cells was compared at 25°C after 3 to 4 days. (C) The *sfh1-1ts* mutation interacts synthetically with the *ndc10-1* mutation. Wild-type (BLY278), *sfh1-1ts* (BLY353), *ndc10-1* (BLY506), and *sfh1-1 ndc10-1* (BLY538) strains were grown on YPD plates at the temperatures indicated for 3 to 4 days. (D) Increased dosage of *CSE4* partially suppresses the temperature sensitivity and TBZ sensitivity of *sfh1-1ts* mutants. Equal numbers of tenfold serially diluted mid-logarithmic-phase *sfh1-1ts* cells (BLY353) carrying YEp24 or YEp24-derived high-copy plasmids expressing *SFH1* (pYC5H), *CSE4* (pPY3), or *NDC10* (pPM47) were spotted onto SC plates lacking uracil and incubated at 25°C or 31°C or onto SC plates lacking uracil plates containing 60 μg of TBZ per ml and incubated at 25°C. Cell growth was compared after 3 to 4 days. (E) *sth1-3ts* mutations cause synergistic chromosome instability when combined with a CDEI but not a CDEII mutation. The stabilities of chromosome fragments containing either a wild-type *CEN* or mutant *CEN* sequence CDEI(8-C) or CDEII(+45) in *STH1* (BLY361, BLY429, and BLY424, respectively) and *sth1-3ts* (BLY360, BLY565, and BLY566, respectively) cells were determined by plating cells onto adenine indicator plates. Cells were grown at 34°C and photographed after 3 to 4 days. Red sectors indicate missegregation of the chromosome fragment.

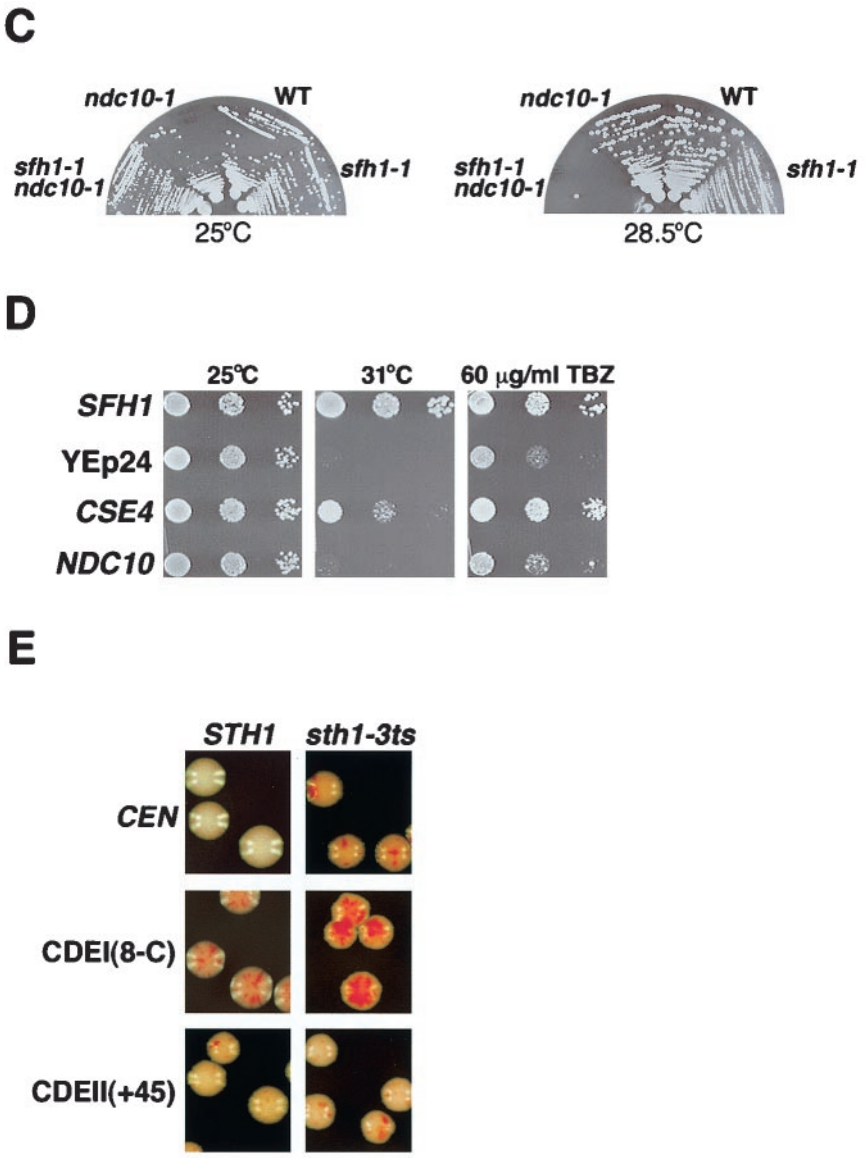

FIG. 2—*Continued.*

1.1×10^{-3}) and no significant change in rates of 1:0 chromosome loss (1.3×10^{-3} versus 0.9×10^{-3}) (Fig. 1B). Thus, chromosome destabilization in *sth1-3ts* mutants occurs predominantly by sister chromatid nondisjunction, consistent with another *sth1* allele (73). These results suggest that cells require RSC for the faithful transmission of chromosomes during mitosis.

***sth1-3ts* and *sfh1-1ts* interact genetically with mutations in both kinetochore components and a centromeric DNA element.** Proper chromosome segregation requires centromeric (*CEN*) DNA and the kinetochore, a protein complex that assembles onto *CEN* DNA to mediate the attachment of chromosomes to the spindle microtubules. The engagement of the spindle checkpoint and the chromosome segregation defects in *rsc* mutants suggest a role for RSC in kinetochore function. To test whether RSC interacts with kinetochores, we constructed double mutants between the *sth1-3ts* or *sfh1-1ts* mutation and mutations in one of the kinetochore genes *CSE4*, *MIF2*, *NDC10*/*CTF14*, and *CTF13*. The *sth1-3ts cse4-1* and *sth1-3ts mif2-3* mutants exhibited conditional synthetic lethality at 35°C, and the *sth1-3ts ndc10-1* and *sth1-3ts ctf14-42* double mutants grew dramatically more slowly than either of the single mutants at semipermissive temperatures (Fig. 2A). All mutant strains grew as well as wild-type cells at the permissive temperature (Fig. 2A; only *ctf14-42* is shown). We also found that *sth1-3ts* combined with either the *cse4-1* or *mif2-3* mutation caused enhanced hypersensitivity to TBZ (Fig. 2B). This suggests that RSC exhibits functionally distinct as well as overlapping roles with kinetochore proteins in microtubule-dependent processes.

Like *sth1-3ts*, the *sfh1-1ts* mutation interacted synthetically with the *ndc10-1* mutation (Fig. 2C), shown previously to pre-

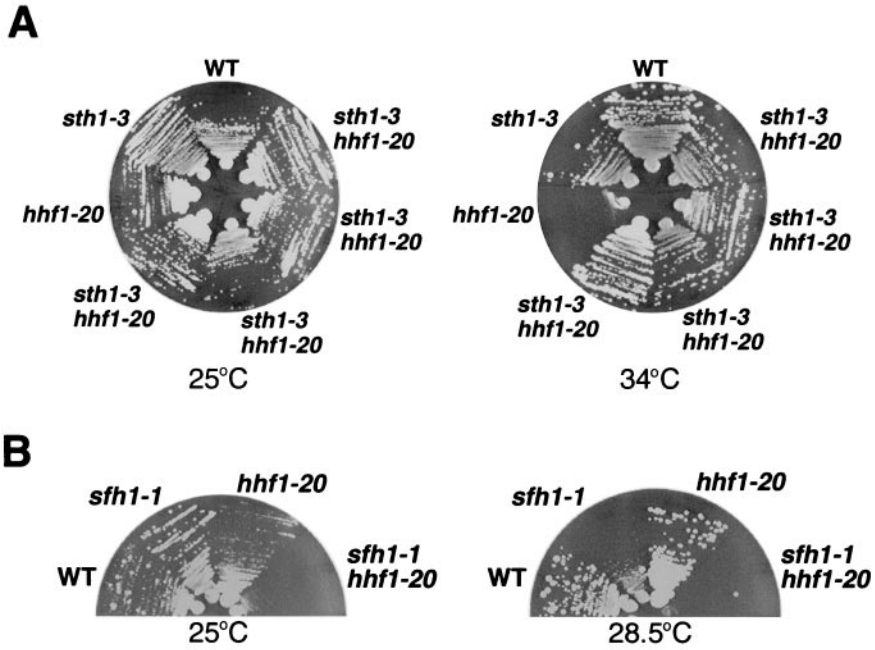

FIG. 3. *sth1-3ts* and *sfh1-1ts* mutations interact with a histone H4 mutation, *hhf1-20*. (A) *sth1-3ts* suppresses the temperature-sensitive phenotype of *hhf1-20* mutants. Growth of *sth1-3ts hhf1-20* double mutants (BLY546) was compared to that of *hhf1-20* (BLY415), *sth1-3ts* (BLY49), and wild-type (WT, BLY76) cells at 25°C and 34°C. Plates were incubated for 2 to 3 days. Four independently isolated double mutant strains were tested. (B) The *sfh1-1ts* mutation combined with *hhf1-20* results in synthetic growth defects. The growth of wild-type (BLY278), *sfh1-1ts* (BLY353), *hhf1-20* (BLY415), and *sfh1-1ts hhf1-20* (BLY552) cells on YPD was compared at the indicated temperatures after 3 days.

vent formation of the CBF3-*CEN* DNA complex in vitro and in vivo (48, 65). In addition, our failure to recover *sfh1-1ts ctf13-30* or *sfh1-1ts cft14-42* double mutants from at least 40 tetrads examined from each strain suggests that these *ctf* mutations are lethal in combination with *sfh1-1ts*.

As *rsc* mutants interacted synthetically with kinetochore mutants, we next tested whether overexpression of kinetochore proteins could suppress the temperature-sensitive (Ts^-) phenotypes of *rsc* mutants. We found that high-copy *CSE4* but not *NDC10*, *MIF2*, or *CBF1* partially suppressed the Ts^- phenotype of *sfh1-1ts* at 31°C (Fig. 2D; only the *CSE4* and *NDC10* data are shown). High-copy *CSE4* also partially suppressed the TBZ sensitivity of *sfh1-1ts* cells (Fig. 2D). Interestingly, a strain bearing a deletion of the homologous *SNF5* gene, which encodes a core component of the Snf-Swi complex, was also sensitive to TBZ, although high-copy *CSE4* was unable to suppress the TBZ sensitivity (data not shown), suggesting that the interaction with centromeric components of the kinetochore is specific to RSC components.

Mutations in genes encoding kinetochore proteins have been shown to enhance chromosome missegregation when combined with mutations in centromere DNA elements (CDEs) (3, 34, 42). For example, chromosomes are lost at unusually high rates in mutants carrying *cse4* mutations plus CDEI or CDEII mutations (34). To determine if RSC interacts with centromeric DNA sequences, we tested whether combining *sth1-3ts* and the CDEI(8-C), CDEII(+45), or CDEII(Δ31) mutation caused synthetic impairment of chromosome segregation. At the semipermissive temperature (34°C), the *sth1-3ts* mutation caused elevated missegregation of a chromosome fragment containing wild-type *CEN* sequences, as described previously above (Fig. 1B), and this missegregation was greatly exacerbated when the chromosome fragment carried the CDEI(8-C) mutation (Fig. 2E). However, neither the *sth1-3ts* CDEII(+45) nor the *sth1-3ts* CDEII(Δ31) double mutant showed higher missegregation rates than the single mutants [Fig. 2E; only CDEII(+45) is shown]. This analysis suggests that RSC interacts with centromeric DNA element CDEI but not with CDEII. Taken together, the genetic interactions between *rsc* and both kinetochore and centromere DNA element mutations strongly imply an important role for RSC in centromere-kinetochore function.

***rsc* interacts with a histone H4 mutation that disrupts centromeric structure and function.** Centromeric chromatin is distinguished by the presence of a histone H3 variant. In humans, equimolar amounts of histones H2A, H2B, and H4 and the histone H3 variant CENP-A assemble to form a specialized nucleosome in vitro (68). Considering the specific genetic interactions between RSC and the Cse4p component of centromeric chromatin and the ability of RSC to remodel nucleosome structure in vitro, we reasoned that *rsc* would interact with *hhf1-20*, a histone H4 mutation that disrupts centromeric chromatin structure and missegregates chromosomes (22, 43, 64). The *hhf1-20* single mutant was unable to grow at 34°C, but its growth was restored in the *sth1-3ts* mutant background. Thus, the *sth1-3ts* mutation suppressed the temperature sensitivity of *hhf1-20* (Fig. 3A). In contrast, the *sfh1-1ts* mutation showed synthetic sickness when combined with the *hhf1-20* mutation, even at the permissive temperature (Fig. 3B). These data suggest that Sth1p and Sfh1p interact differently with centromeric histones and are consistent with the differential cross-linking of these proteins to nucleosomes (57). One pos-

sibility is that individual RSC subunits contribute differently to the distinct chromatin-remodeling activities of RSC (e.g., histone octamer transfer and nucleosome sliding) (39).

Sth1p interacts directly with the histone H3 variant Cse4p and histones H3, H4, and H2B. A prediction from the genetic interactions observed in combining *rsc* and kinetochore component mutations is that RSC interacts physically with these proteins. We investigated the ability of Sth1p to interact with the kinetochore components Ndc10p, Ctf19p, Mif2p, and Cse4p in the yeast two-hybrid assay. Sth1p fused to the LexA DNA-binding domain interacted with Cse4p fused to the Gal4p activation domain but not with the other kinetochore components when β-galactosidase activity was analyzed in the reporter strain (Fig. 4A). The interaction was slightly weaker than that between Sth1p and a second conserved RSC component, Rsc8p (71). Thus, Sth1p interacts specifically with a histone component of centromeric chromatin.

We tested further whether Sth1p interacts with histones in vivo by immunoprecipitation. We found that Sth1p specifically coprecipitated with Flag-H2B when anti-Flag antibodies were used. Sth1p also interacted with Flag-H2B in immunoprecipitations with anti-Sth1p antibody (data not shown). In the presence of DNase I, Sth1p still associated with Flag-H2B, although at a slightly reduced level (Fig. 4B, compare lanes 4 and 6). Similarly, Sth1p also immunoprecipitated with Flag-tagged histones H3 and H4 in the presence of DNase I (bottom two panels, compare lanes 3 and 4), suggesting that these interactions occurred through protein-protein interactions. However, these experiments do not distinguish whether these interactions occur directly through Sth1p or through another protein(s).

We further investigated the interactions between Sth1p and histones by Far-Western and GST pulldown analyses. In vitro-translated Sth1p bound specifically and strongly to histones H3 and H4 and to histone H2B but not detectably to histone H2A (Fig. 4C). The lack of a significant signal with H2A suggests that the Sth1p interactions with H3, H2B, and H4 are specific and not due simply to electrostatic interactions. In addition, we showed that Sth1p bound to the N-terminal tails of histones H3 (amino acids 1 to 46) and H4 (amino acids 1 to 34) (Fig. 4D, upper and lower panels, lane 3) in GST pulldown assays. Interestingly, Sth1p interacted specifically with amino acids 1 to 25 of histone H3 (Fig. 4D, upper panel, compare lanes 4 and 5) and residues 15 to 34 of histone H4 (Fig. 4D, lower panel, compare lanes 4 and 5). These selective interactions with specific regions of histone tails may have important implications for the mechanism of RSC remodeling.

RSC localizes to centromeric and flanking chromatin in vivo. The genetic and physical interactions between RSC and kinetochore components are consistent with a functional role for RSC at or near the centromere. Thus, we investigated the association of RSC with centromere and centromere-proximal DNAs in vivo by monitoring the presence of functional hemagglutinin (HA)-tagged Rsc8p in the chromatin immunoprecipitation assay. Like Mcd1p, a subunit of cohesin, Rsc8p-HA protein interacts with centromeric DNA in vivo. In addition to its presence at the centromere of chromosome XVI (*CEN16*), Rsc8p-HA was also present at centromere-proximal regions at distances 2.5 kb and 4.0 kb 3′ to CDEIII of *CEN3* but not at a Ty element ≈30 kb 5′ to CDEI of *CEN3* (Fig. 5A). As cohesin has been shown to localize to centromeric and centromere-flanking sequences (7, 69), we sought to determine the localization pattern for RSC in this region. We found that RSC was associated with the contiguous 4.0-kb regions on either side of *CEN3* (data not shown). Nearly identical localization patterns for RSC were observed whether Sth1p-HA or Sfh1p-HA strains were used (data not shown). To determine if the presence of RSC at centromeric chromatin is cell cycle dependent, we synchronized cells in the S and G_2/M phases of the cell cycle. RSC was associated with the centromere of chromosome I (*CEN1*) and the centromere-proximal region 0.28 kb 3′ to CDEIII of *CEN3* in both cell cycle stages (Fig. 5B).

We next examined whether the association of RSC with chromosomal DNA is dependent on functional Sth1p by comparing the enrichment of *CEN* and flanking DNAs in *sth1-3ts* cells grown at the permissive and nonpermissive temperatures. The levels of immunoprecipitated DNAs in *sth1-3ts* cells grown at 37°C were greatly reduced compared to those in mutant strains grown at 25°C and wild-type cells at either 25°C or 37°C (Fig. 5C, compare lane 8 with lane 7 and lane 7 with lanes 3 and 4). The reduced association was not due to decreased Sth1p levels or DNA inputs, as both the levels of Sth1p that coimmunoprecipitated with Rsc8p-HA and the initial DNA inputs for chromatin immunoprecipitation assays were comparable in the mutant and wild-type strains at both temperatures (data not shown). We infer that Sth1p is required for recruitment or stable association of RSC with chromosomal loci. Interestingly, Sth1p is one of three RSC components that is cross-linked to nucleosomal DNA prior to remodeling (57). These results suggest that RSC function is required at both centromeric and flanking chromosomal regions.

Centromeric chromatin structure is altered in *rsc* mutants. To test whether RSC function is required for the proper configuration of centromeric chromatin, we analyzed the centromeric and adjacent chromatin structure of *CEN3* in *rsc* mutants with both the endonuclease accessibility assay and indirect end-labeling analysis of MNase-digested chromatin. The three *Dra*I restriction sites in the CDEII region of *CEN3* are normally protected from endonuclease digestion, presumably due to the presence of the centromere-kinetochore protein complex. Mutations in *CEN* DNA or kinetochore components as well as depletion of histones H2B or H4 were previously shown to increase the accessibility of CDEII to *Dra*I endonuclease digestion (54, 55).

The *Dra*I sites within CDEII of *CEN3* remained inaccessible in wild-type cells grown at 35°C and in *sth1-3ts* mutants grown at the permissive temperature (25°C). However, upon shifting mutants to 35°C, *Dra*I accessibility increased dramatically in *sth1-3ts* mutants (Fig. 6A). This increase in accessibility resembled that in *hhf1-20* mutants, whose mutation was previously shown to cause centromeric chromatin structural alterations (43).

We next examined the centromeric chromatin structure around *CEN3* in *sfh1-1ts* mutants by indirect end labeling of MNase-digested chromatin. Both *SFH1* and *sfh1-1ts* cells showed ordered nucleosome arrays flanking the *CEN3* nuclease-resistant centromeric core (8, 51). At both the permissive (25°C) and nonpermissive (37°C) temperatures, the MNase digestion patterns of chromatin in wild-type *SFH1* cells were comparable. However, the pattern was altered in *sfh1-1ts* mu-

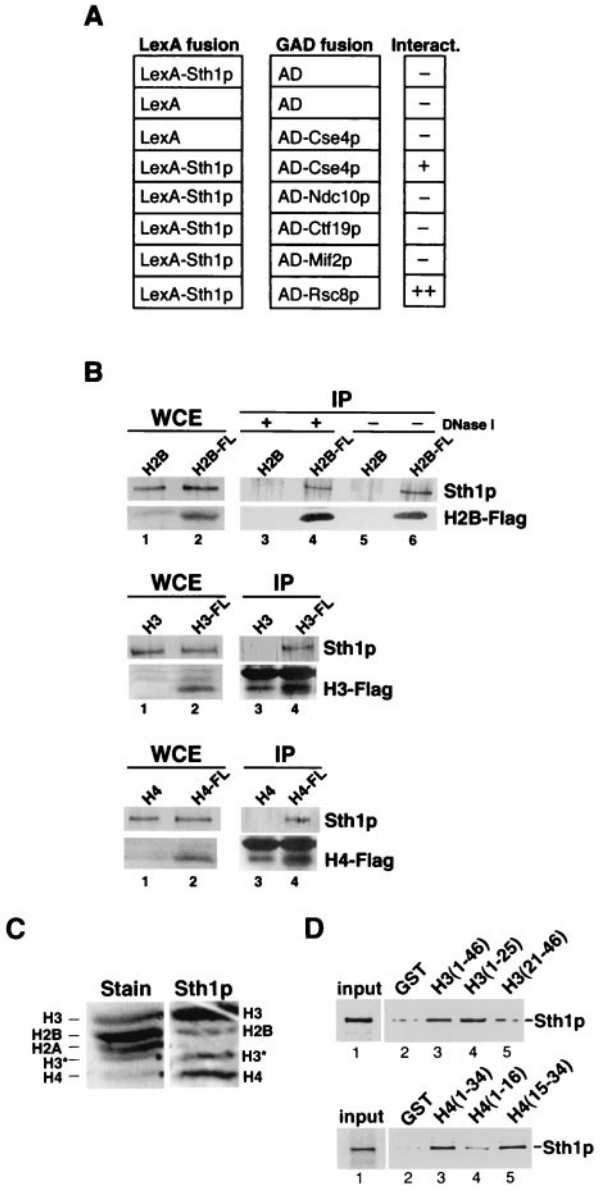

FIG. 4. Sth1p interacts physically with the histone H3 variant Cse4p and histones H3, H4, and H2B. (A) Sth1p interacts with Cse4p in the yeast two-hybrid assay. β-Galactosidase activity was assayed in the *lexAop-lacZ* (BLY2) reporter strain expressing pLexA or pLexA$_{202}$-Sth1$_{1-1359}$ and Gal4p activation domain (GAD) or GAD fusion proteins expressed from pACT2, pJL484, pJL486, pJO196, pGAD-CTF19, or pIT331. β-Galactosidase activity in permeabilized cells was determined as described previously (11). No significant interactions were detected in cells expressing the LexA DNA-binding partner alone and GAD fusion proteins or in cells expressing the GAD activating partner alone and LexA$_{202}$-Sth1$_{1-1359}$. The interaction between LexA$_{202}$-Sth1$_{1-1359}$ and GAD-Cse4p was confirmed in β-galactosidase liquid assays (data not shown). AD, activation domain. (B) Sth1p interacts with Flag-tagged histones H2B, H3, and H4 in vivo. Anti-Flag M2 monoclonal antibody affinity resin was incubated with whole-cell extracts (WCE) prepared from cells carrying plasmids expressing Flag-H2B (BLY309), H2B (BLY283), Flag-H3 (BLY573), or Flag-H4 (BLY575) and cells carrying pRS315 (BLY572) and pRS425 (BLY574) as controls for Flag-H3 and Flag-H4, respectively. Immune complexes were separated on SDS–4 to 20% polyacrylamide gradient or SDS–15% acrylamide gels and immunoblotted with anti-Sth1p (1:1,000) polyclonal or anti-Flag M2 (1:300) monoclonal antibodies. Lanes 1 and 2, 1/83 of input lysate for both anti-Sth1p and anti-Flag immunoblots; lanes 3, 4, 5, and 6, entire immunoprecipitation pellets for both anti-Sth1p and anti-Flag Western blots. Immunoprecipitations (IPs) were performed in the presence of 250 U of DNase I except for lanes 5 and 6, from which DNase I was omitted. Nonspecific proteins comigrated with immunoprecipitated Flag-H3 and Flag-H4 proteins (compare lanes 3 and 4). (C) Sth1p interacts directly with histones H3, H4, and H2B by Far-Western analysis. Samples of acid-soluble enriched histones were separated by SDS–21% PAGE, blotted to polyvinylidene difluoride membranes, and probed with radiolabeled Sth1p (Sth1p). A parallel lane of transferred histones was stained with Ponceau S (Stain). H3* is a spontaneous breakdown product of histone H3. (D) Sth1p interacts directly with the N termini of histones H3 and H4. [^{35}S]methionine-labeled Sth1p was incubated with GST (lanes 2) or GST fusion proteins containing the N termini of histone H3 (amino acids 1 to 46) or H4 (amino acids 1 to 34) (lanes 3), H3 (1 to 25) or H4 (1 to 16) (lanes 4), or H3 (21 to 46) or H4 (15 to 34) (lanes 5) (28) immobilized on glutathione-Sepharose beads. We analyzed 25% of the input fractions and 100% of the bound and unbound fractions by SDS–8% PAGE, and labeled Sth1p was visualized by PhosphorImager analysis. Similar results were observed in at least four independent experiments.

tants, and this change was most evident at 37°C. The levels of MNase digestion between nucleosomes were diminished at two positions in the region 5′ to CDEI (Fig. 6B, compare lanes 17 and 13 with lanes 9 and 5). Interestingly, we did not observe any significant differences in the MNase digestion pattern between the wild-type and the *sfh1-1ts* mutant 3′ to CDEIII (data not shown). Taken together, these results indicate that the core centromeric chromatin and flanking chromatin structures are significantly altered in *rsc* mutants.

Kinetochore components remain associated with the centromere in *sth1-3ts* mutants. One explanation for the *rsc* mutant defects in centromeric chromatin structure and chromosome segregation is that kinetochore proteins or proteins necessary for centromeric cohesion are not deposited properly at centromeres. To test this, we assessed binding of Mif2p and Cse4p-3HA to *CEN3* DNA by chromatin immunoprecipitation analysis of chromatin prepared from wild-type and *sth1-3ts* cells grown at the permissive (23°C) and nonpermissive (37°C) temperatures by chromatin immunoprecipitation analysis. Comparable levels of *CEN3* DNAs were immunoprecipitated in each case from *sth1-3ts* cells at 23°C and 37°C (Fig. 7; lower panel, compare lanes 4 through 7 to lanes 11 through 14, respectively), and these levels were similar to those in wild-type cells grown under the same conditions (compare upper and lower panels, lanes 4 through 7 and lanes 11 through 14, respectively). These results suggest that RSC is not required for localization of these proteins to the kinetochore.

***rsc* mutants are defective in sister chromatid segregation.** The structural alterations of centromeric chromatin and missegregation of a chromosome fragment in *rsc* mutants are consistent with defects in several aspects of chromosome segregation, including kinetochore assembly, sister kinetochore biorientation, sister chromatid cohesion, and the dynamic oscillatory movements of chromatids prior to the onset of anaphase. To more directly assess chromosome behavior in *rsc* mutants, we followed sister chromatid segregation with GFP-TetR-marked chromosomes tagged either 206 bp from *CEN1* or 35 kb from *CEN5* on the left arm of chromosome V.

Sister chromatids marked at *CEN1* exhibited obvious segregation defects in *sth1-3ts* mutant cells shifted to 37°C for 8 h.

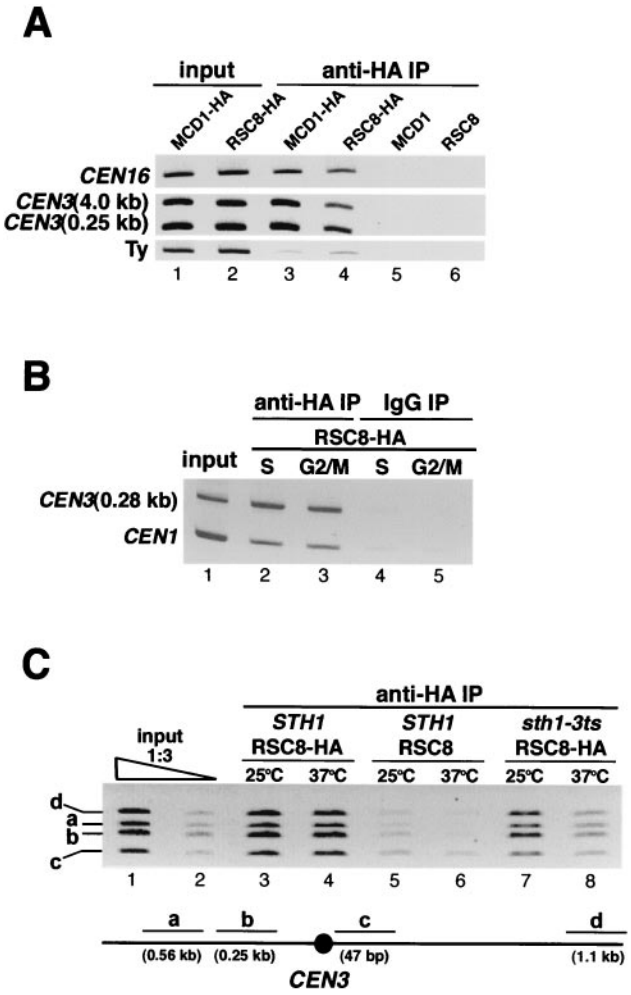

FIG. 5. Rsc8p associates with centromeric and flanking chromosomal regions in vivo. (A) Rsc8p is localized to centromeric and flanking regions. Chromatin prepared from extracts of cells expressing Mcd1p-HA (BLY397) or Rsc8p-HA (BLY298), and untagged Mcd1p (BLY398) or Rsc8p (BLY301) grown to mid-logarithmic phase in YPD was immunoprecipitated (IP) with anti-HA antibodies. Coimmunoprecipitated DNAs were amplified by PCR with primers specific for the indicated chromosomal loci. (B) Rsc8p localizes to *CEN3*-flanking and *CEN1* regions in S- and G_2/M-phase-synchronized cells. Chromatin was prepared from cells expressing HA-tagged Rsc8p (BLY298) synchronized in S or G_2/M phase by treatment with hydroxyurea or nocodazole, respectively, for 3 h at 25°C. (C) Association of Rsc8p with *CEN* DNA and flanking regions is defective in *sth1-3ts* mutants. Chromatin was prepared from mid-logarithmic-phase RSC8-HA (BLY298), RSC8 (BLY301), and *sth1-3ts* RSC8-HA (BLY549) cells grown at 25°C or 37°C for 8 h. A schematic map showing the positions of the PCR products relative to *CEN3* is shown.

Among large-budded cells with two GFP dots within one cell body, 36% were accompanied by bilobed or binucleated DNA masses within the same cell body, and 7% exhibited an uncoupling of bulk DNA segregation from sister chromatid segregation (Fig. 8A, columns b and c). Even in the remaining 54% of cells in which two sister chromatids separated within a single DNA mass, the nucleus was frequently positioned away from the mother bud neck (Fig. 8A, column d). Examination of mitotic spindles in *sth1-3ts* mutants by labeling microtubules with GFP-Tub1p revealed that while the majority of large-budded cells with a single nucleus contained characteristically short spindles, a subpopulation of mutants with either single or separated DNA masses contained aberrant spindles. In cells with a single DNA mass, the spindle was frequently elongated and incorrectly positioned compared to wild-type cells in similar cell cycle stages (Fig. 8B, compare column b with column a). In cells containing two separated DNA masses within the same cell body, the spindles were entirely contained within the mother cell. The middle portions of these spindles were often not visible (Fig. 8B, column c). Thus, the chromosome segregation defects in *rsc* mutants could result from defects in both kinetochore and microtubule functions.

Interestingly, when chromosome arms were marked 35 kb from *CEN5*, we observed sister chromatid separation within single nuclear DNA masses in arrested mutants (Fig. 8A, column e). This was unexpected because chromosome arms in wild-type cells do not normally undergo transient separation prior to the onset of segregation. Similar separation defects were also observed in *sfh1-1ts* cells with chromosomes tagged 35 kb from *CEN5* (data not shown).

To further explore the chromosome missegregation phenotype in *rsc* mutants, wild-type and *sth1-3ts* mutant cells marked at *CEN1* were arrested in G_1 with α-factor and then released to study sister chromatid separation and segregation in synchronous cells. Wild-type and *sth1-3ts* mutant cells showed similar budding kinetics following release from α-factor. At 60 min following release, both wild-type and mutant cells had similar percentages of budded cells with single GFP dots. As cells progressed through the cell cycle, the population of wild-type cells with segregated sister chromatids increased. In contrast, in the *sth1-3ts* mutants, the percentage of cells with segregated chromatids remained low. Instead, the population of cells with two separated but not segregated sister chromatids increased. For example, 100 min following release, 57% of the wild-type cells and only 27% of *sth1-3ts* mutant cells had segregated their sister chromatids (Fig. 8C, black bars). While the percentages of wild-type and mutant cells with single GFP-*CEN1* fluorescent dots was comparable (36% versus 35%; gray bars), there was a significant increase in *sth1-3ts* mutants with separated sister chromatids in one cell body (38% versus 6%; open bars). Accumulation of separated but not segregated sister chromatids in *sth1-3ts* cells might result from activation of the spindle checkpoint and is consistent with our previous genetic and structural analyses.

DISCUSSION

In this study, we present several lines of evidence that RSC function is required at the kinetochore during chromosome segregation. First, the *sth1* and *sfh1* mutations interact genetically with mutations in kinetochore components, centromeric histones, and centromeric DNA elements. Second, RSC is localized to centromeric and centromere-flanking chromatin and interacts genetically and physically with histone and histone variant components of chromatin. Finally, centromeric nucleosome structure is altered and TetR-GFP-tagged chromosomes are missegregated in both *sth1* and *sfh1* mutants. These data suggest a model in which the RSC ATP-dependent remodeling complex is required to restructure centromeric and

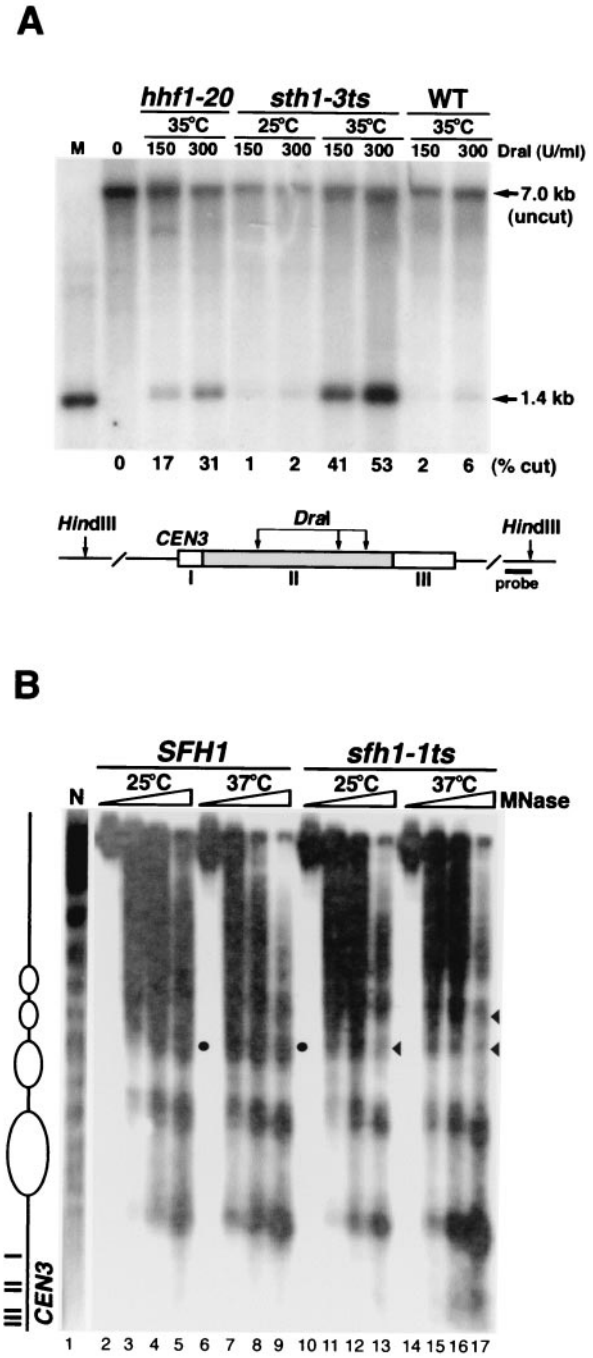

FIG. 6. Centromeric and flanking chromatin structure is altered in *rsc* mutants. (A) *Dra*I accessibility to CDEII of *CEN3* is increased in *sth1-3ts* mutants. Nuclei isolated from *sth1-3ts* (BLY49) grown at 25°C or *hhf1-20* (BLY413), *sth1-3ts* (BLY49), and wild-type (WT, BLY76) cells grown at 35°C for 8 h were first digested with *Dra*I. Southern blot analysis of the purified DNA subsequently digested with *Hin*dIII is shown. M, ≈1.4-kb *Dra*I-*Hin*dIII genomic fragment as a marker. The 7.0-kb band is the intact *Hin*dIII fragment uncut by *Dra*I. The fraction of CDEII chromatin digested by *Dra*I is shown as a percentage. (B) Pericentromeric chromatin structure is altered in the *sfh1-1ts* mutant. Indirect end labeling of micrococcal nuclease-digested chromatin prepared from *SFH1* (BLY278) and *sfh1-1ts* (BLY353) cells grown at 25°C or 37°C for 8 h. CDEI-proximal pericentromeric chromatin structure is shown. The arrowheads indicate regions in the mutant with altered digestion patterns; solid circles indicate the corresponding regions in wild-type cells. N, naked DNA control.

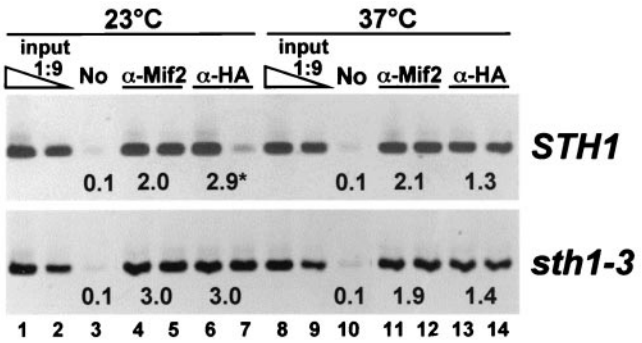

FIG. 7. Mif2p and Cse4p remain associated with centromeres in *sth1-3ts* mutant cells. Chromatin was prepared from extracts of wild-type *STH1* or mutant *sth1-3ts* cells expressing HA-tagged Cse4p (PM1311 and PM1312, respectively). Cells grown to mid-logarithmic phase in YPD medium at 23°C were first incubated with α-factor for 3 h to arrest cells in G_1 phase (≈85%). Half of each culture was then shifted to 37°C in the continued presence of α-factor for 30 min, after which cells were washed with YPD containing 0.1 mg of pronase per ml at 23°C or 37°C and released into fresh YPD medium containing 0.1 mg of pronase per ml and nocodazole. Cells were incubated for an additional 3.5 h before processing for chromatin immunoprecipitation. Duplicate stained *CEN3* PCR products (except for lane 7, upper panel) were imaged and quantified. No, mock immunoprecipitation without antibody.

centromere-flanking nucleosome structure for the accurate transmission of chromosomes.

Both genetic and biochemical data support direct interactions between RSC and Cse4-containing nucleosomes at kinetochores. Processes that may require such interactions include the recruitment, assembly, and maintenance of Cse4-containing nucleosomes. The ability of Cse4p to associate with centromeric DNA in *sth1-3ts* mutants suggests that the recruitment of Cse4p to kinetochores does not require RSC. However, the alterations in centromeric chromatin structure in *rsc* mutants suggest that RSC could function at kinetochores in the postrecruitment assembly or maintenance of centromeric chromatin. One model is that RSC functions early in centromeric nucleosome assembly, possibly with factors such as CAF-1/Hir1 (58), during which Cse4p is postulated to compete with histone H3 for binding to histone H4 (22, 43). We found that high-copy Cse4p could partially suppress both the Ts^- and TBZ sensitivity phenotypes of *sfh1-1ts* mutants. Presumably, compromised RSC function would result in a shifted balance between Cse4/H4 and H3/H4 assembly in *sfh1-1ts* mutants. High-dosage *CSE4* would then suppress the *sfh1-1ts* mutation by driving assembly of Cse4p/H4. Alternatively, RSC could promote the proper positioning of Cse4p-containing nucleosomes on centromeric DNA. During S phase, centromeres of all chromosomes are clustered near spindle pole bodies (33). Recruitment of Cse4p could result in high local concentrations of Cse4p that spread to immediate adjacent regions, similar to what has been observed in experiments in which human CENP-A was overexpressed (75). Thus, the transfer of these ectopic Cse4p-containing nucleosomes catalyzed by RSC would ensure their proper association with centromeric DNA. RSC could catalyze the sliding of Cse4p-containing octamers to finely adjust their positions relative to CDEs, a role that would be especially important in the G_2/M phase, when microtubules attach to kinetochores and pull the sister chroma-

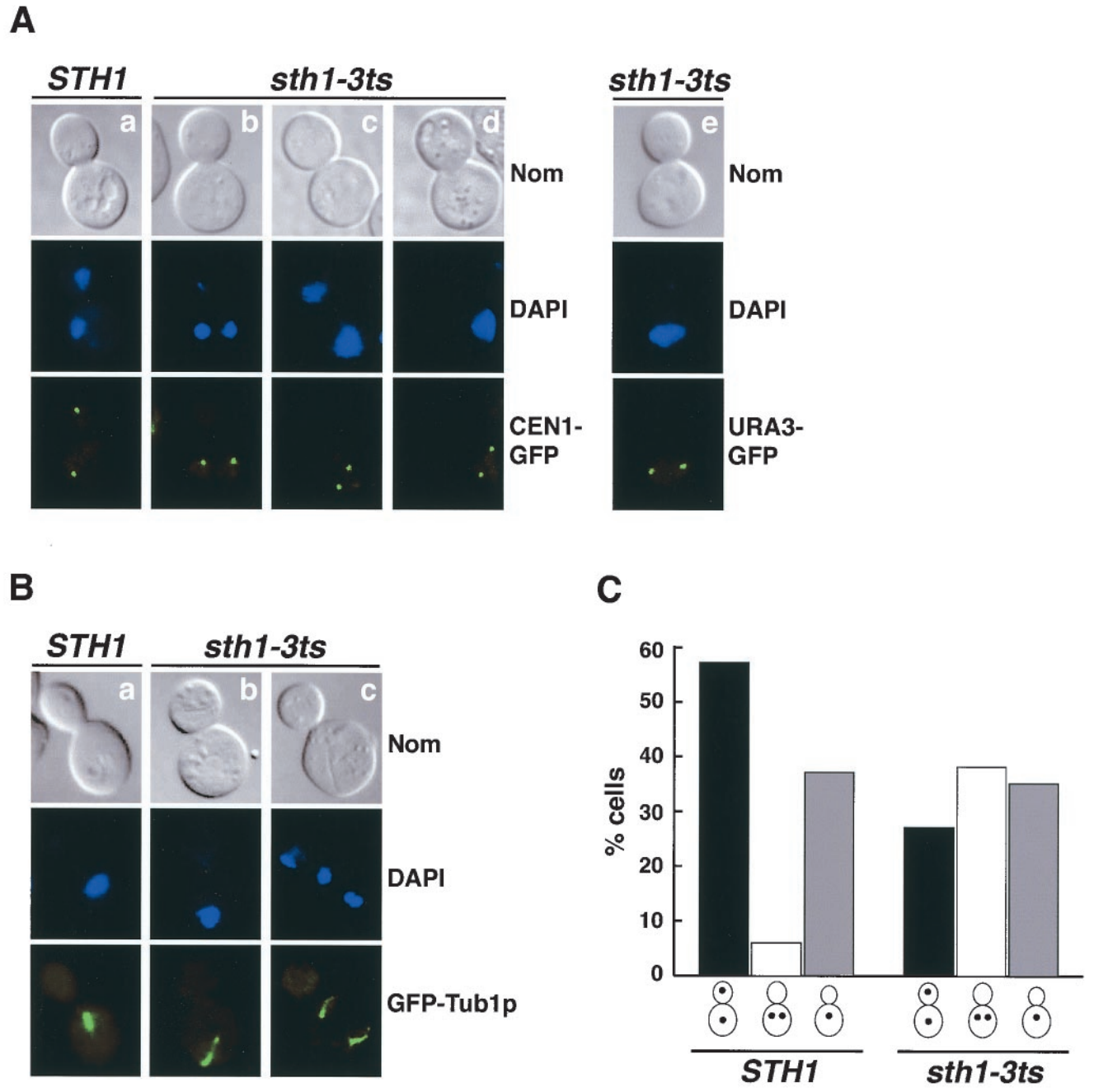

FIG. 8. *rsc* mutants missegregate authentic chromosomes. (A) Sister chromatid segregation is defective in *sth1-3ts* mutants. *STH1* (BLY520) and *sth1-3ts* (BLY526) cells marked at *CEN1* were grown to mid-logarithmic phase at 25°C, diluted, and shifted to 37°C for 8 h. Representative mutant cells with separated sister chromatids in one cell body are shown (columns b to d). Mutant *sth1-3ts* cells (BLY493) marked at *URA3* (35 kb from *CEN5*) with separated sister chromatids are shown in column e. Nuclei were visualized by 4,6-diamidino-2-phenylindole (DAPI) staining. Nom, Nomarski images. (B) Spindle morphology is aberrant in *sth1-3ts* mutants. Mid-logarithmic-phase wild-type (BLY570) and *sth1-3ts* (BLY568) cells expressing the GFP-Tub1p fusion protein were grown at 37°C for 8 h. Microtubule structures were analyzed by fluorescence microscopy. (C) Sister chromatid segregation is delayed in *sth1-3ts* cells. Wild-type (BLY520) and *sth1-3ts* (BLY526) strains marked at *CEN1* were arrested in G_1 with α-factor, released at 37°C, and scored for sister chromatid separation and segregation. The percentages of cells with segregated, separated, and unseparated sister chromatids 100 min after α-factor release are plotted.

tids apart. Proper positioning of the Cse4p-containing nucleosomes relative to the centromeric DNA sequences provides important structural support for the overall configuration and function of kinetochores.

Although our chromosome tagging experiments revealed that kinetochore-microtubule interactions are largely intact in *rsc* mutants, these *rsc* mutations were found to activate the *MAD1*-dependent spindle checkpoint. Thus, subtle alterations

of centromeric chromatin could nevertheless impact microtubule-kinetochore function in chromosome segregation. Recent studies have identified several protein complexes that function at the kinetochore. Assembly of the kinetochore involves the initial binding of CBF3 to CDEIII, followed by additional protein-protein and protein-*CEN* DNA interactions (14). Centromeric DNA conformation is also important for facilitating protein-protein interactions at the kinetochore (48). Interestingly, the *sth1-3ts* and *mif2* mutations show similar genetic interactions with CDEI but not CDEII mutations. Thus, RSC could facilitate the bending of centromeric DNA for kinetochore assembly, as has been proposed for Mif2p (9, 41, 42, 48). The centromeric chromatin structural changes in *rsc* mutants could reflect altered positions of Cse4-containing nucleosomes relative to centromeric DNA or instead alterations in the overall structural configuration of the kinetochore.

RSC also localizes to centromere-proximal regions, suggesting additional roles for RSC in maintaining the structure of this region that is necessary to support kinetochore function. Indeed, centromere-proximal chromatin structure is perturbed in both *sfh1-1ts* and *sth1/nps1-105* mutants (73; this study). Interestingly, Rsc2p is required to maintain the correct nucleosome structure of the STB plasmid locus for 2μm plasmid partitioning (77), a process that likely shares host factors necessary for chromosome segregation (40). Centromere-proximal regions up to 10 to 13 kb on either side of the CDEs undergo dynamic structural changes before kinetochores establish stable bipolar interactions with the mitotic spindle (23, 27, 49). These changes in centromere-proximal higher-order chromatin structure may reflect the localized condensation and decondensation of chromosomes. We envision that RSC is required to remodel flanking nucleosomes throughout these oscillatory chromosome movements to facilitate kinetochore-microtubule interactions. At the same time, RSC, cohesin, and other factors may be coordinately regulated to limit these changes to a range of 10 to 13 kb surrounding the centromere. In both *rsc* mutants, sister chromatid separation occurred when chromosomes were marked 35 kb from *CEN5*, beyond the 10- to 13-kb limit for transient sister separation (49). Although these data support a role for RSC in remodeling centromere-proximal chromatin for kinetochore function, we cannot rule out the possibility that chromosome condensation and/or cohesion is defective in *rsc* mutants, as both local chromatin changes and the reorganization of chromatin by condensin/cohesin could contribute to reversible centromeric chromatin changes (46).

In this study, we have shown that RSC associates with centromeric and centromere-flanking chromatin and functions in chromosome segregation. Recent genome-wide chromatin immunoprecipitation studies have localized RSC to several other chromosomal loci (15, 47). Together, these results imply distinct functions for RSC in chromosome segregation and other cellular processes such as transcription. The dynamic structural changes at centromeric and centromere-flanking regions are likely to involve multiple chromatin-modifying activities. Indeed, in *Schizosaccharomyces pombe* and *Drosophila melanogaster*, histone deacetylase and methyltransferase activities are required for heterochromatic centromere structure and function (5, 6, 16, 19, 50). Like RSC, the related human SWI/SNF-B complex is localized to kinetochores (78). Therefore, at least two classes of chromatin-remodeling complexes may function coordinately at the kinetochore. Interestingly, another human ATP-dependent chromatin-remodeling complex was recently shown to load cohesin onto chromosomes (24). Thus, it appears likely that these remodeling activities function in conjunction with cohesins, condensins, and other factors that regulate local centromeric and centromere-proximal chromatin structure for chromosome segregation. Further investigation is necessary to elucidate the mechanisms by which ATP-dependent remodelers contribute to chromosome transmission.

ACKNOWLEDGMENTS

We thank K. Bloom, D. Burke, M. Carlson, M. Grunstein, P. Hieter, D. Koshland, J. Lechner, P. Megee, A. Murray, M. A. Osley, I. Pinto, E. Tsuchiya, F. Winston, and E. Yeh for generous gifts of plasmids and/or strains, N. Azizian for contributions to Fig. 4, M. Ruiz-Noriega for contributions to Fig. 7, and M. Braunstein for assistance with *CSE4* suppression experiments. Laurent laboratory members F. Geng and B. Chai are thanked for helpful comments on the manuscript.

This work was supported by Public Health Service grant GM56700 from the NIH.

REFERENCES

1. **Amon, A.** 1999. The spindle checkpoint. Curr. Opin. Genet. Dev. **9:**69–75.
2. **Angus-Hill, M. L., A. Schlichter, D. Roberts, H. Erdjument-Bromage, P. Tempst, and B. R. Cairns.** 2001. A Rsc3/Rsc30 zinc cluster dimer reveals novel roles for the chromatin remodeler RSC in gene expression and cell cycle control. Mol. Cell **7:**741–751.
3. **Baker, R. E., K. Harris, and K. Zhang.** 1998. Mutations synthetically lethal with cep1 target S. cerevisiae kinetochore components. Genetics **149:**73–85.
4. **Becker, P. B., and W. Horz.** 2002. ATP-dependent nucleosome remodeling. Annu. Rev. Biochem. **71:**247–273.
5. **Berger, S. L.** 2001. The histone modification circus. Science **292:**64–65.
6. **Bjerling, P., R. A. Silverstein, G. Thon, A. Caudy, S. Grewal, and K. Ekwall.** 2002. Functional divergence between histone deacetylases in fission yeast by distinct cellular localization and in vivo specificity. Mol. Cell. Biol. **22:**2170–2181.
7. **Blat, Y., and N. Kleckner.** 1999. Cohesins bind to preferential sites along yeast chromosome III, with differential regulation along arms versus the centric region. Cell **98:**249–259.
8. **Bloom, K. S., and J. Carbon.** 1982. Yeast centromere DNA is in a unique and highly ordered structure in chromosomes and small circular minichromosomes. Cell **29:**305–317.
9. **Brown, M. T., L. Goetsch, and L. H. Hartwell.** 1993. MIF2 is required for mitotic spindle integrity during anaphase spindle elongation in Saccharomyces cerevisiae. J. Cell Biol. **123:**387–403.
10. **Cairns, B. R., Y. Lorch, Y. Li, M. Zhang, L. Lacomis, H. Erdjument-Bromage, P. Tempst, J. Du, B. Laurent, and R. D. Kornberg.** 1996. RSC, an essential, abundant chromatin-remodeling complex. Cell **87:**1249–1260.
11. **Cao, Y., B. R. Cairns, R. D. Kornberg, and B. C. Laurent.** 1997. Sfh1p, a component of a novel chromatin-remodeling complex, is required for cell cycle progression. Mol. Cell. Biol. **17:**3323–3334.
12. **Carbon, J.** 1984. Yeast centromeres: structure and function. Cell **37:**351–353.
13. **Chai, B., J.-M. Hsu, J. Du, and B. C. Laurent.** 2002. Yeast RSC function is required for organization of the cellular cytoskeleton via an alternative *PKC1* pathway. Genetics **161:**575–584.
14. **Cheeseman, I. M., D. G. Drubin, and G. Barnes.** 2002. Simple centromere, complex kinetochore: linking spindle microtubules and centromeric DNA in budding yeast. J. Cell Biol. **157:**199–203.
15. **Damelin, M., I. Simon, T. I. Moy, B. Wilson, S. Komili, P. Tempst, F. P. Roth, R. A. Young, B. R. Cairns, and P. A. Silver.** 2002. The genome-wide localization of Rsc9, a component of the RSC chromatin-remodeling complex, changes in response to stress. Mol. Cell **9:**563–573.
16. **Dillon, N., and R. Festenstein.** 2002. Unravelling heterochromatin: competition between positive and negative factors regulates accessibility. Trends Genet. **18:**252–258.
17. **Du, J., I. Nasir, B. K. Benton, M. P. Kladde, and B. C. Laurent.** 1998. Sth1p, a *Saccharomyces cerevisiae* Snf2p/Swi2p homolog, is an essential ATPase in RSC and differs from Snf/Swi in its interactions with histones and chromatin-associated proteins. Genetics **150:**987–1005.
18. **Edmondson, D., M. Smith, and S. Roth.** 1996. Repression domain of the yeast global repressor Tup1 interacts directly with histones H3 and H4. Genes Dev. **10:**1247–1259.
19. **Ekwall, K., T. Olsson, B. M. Turner, G. Cranston, and R. C. Allshire.** 1997. Transient inhibition of histone deacetylation alters the structural and functional imprint at fission yeast centromeres. Cell **91:**1021–1032.
20. **Fyodorov, D. V., and J. T. Kadonaga.** 2001. The many faces of chromatin remodeling: SWItching beyond transcription. Cell **106:**523–525.

21. **Geng, F., Y. Cao, and B. C. Laurent.** 2001. Essential roles of Snf5p in Snf-Swi chromatin remodeling in vivo. Mol. Cell. Biol. **21:**4311–4320.
22. **Glowczewski, L., P. Yang, T. Kalashnikova, M. S. Santisteban, and M. M. Smith.** 2000. Histone-histone interactions and centromere function. Mol. Cell. Biol. **20:**5700–5711.
23. **Goshima, G., and M. Yanagida.** 2000. Establishing biorientation occurs with precocious separation of the sister kinetochores, but not the arms, in the early spindle of budding yeast. Cell **100:**619–633.
24. **Hakimi, M. A., D. A. Bochar, J. A. Schmiesing, Y. Dong, O. G. Barak, D. W. Speicher, K. Yokomori, and R. Shiekhattar.** 2002. A chromatin remodelling complex that loads cohesin onto human chromosomes. Nature **418:**994–998.
25. **Han, M., M. Chang, U. J. Kim, and M. Grunstein.** 1987. Histone H2B repression causes cell-cycle-specific arrest in yeast: effects on chromosomal segregation, replication, and transcription. Cell **48:**589–597.
26. **Hanes, S. D., and R. Brent.** 1989. DNA specificity of the bicoid activator protein is determined by homeodomain recognition helix residue 9. Cell **57:**1275–1283.
27. **He, X., S. Asthana, and P. K. Sorger.** 2000. Transient sister chromatid separation and elastic deformation of chromosomes during mitosis in budding yeast. Cell **101:**763–775.
28. **Hecht, A., T. Laroche, S. Strahl-Bolsinger, S. Gasser, and M. Grunstein.** 1995. Histone H3 and H4 N-termini interact with SIR3 and SIR4 proteins: a molecular model for the formation of heterochromatin in yeast. Cell **80:**583–592.
29. **Hegemann, J. H., and U. N. Fleig.** 1993. The centromere of budding yeast. Bioessays **15:**451–460.
30. **Hieter, P., C. Mann, M. Snyder, and R. W. Davis.** 1985. Mitotic stability of yeast chromosomes: a colony color assay that measures nondisjunction and chromosome loss. Cell **40:**381–392.
31. **Hurley, J. L., and J. E. Donelson.** 1980. Nucleotide sequence of the yeast plasmid. Nature **286:**860–865.
32. **Hyman, A. A., and P. K. Sorger.** 1995. Structure and function of kinetochores in budding yeast. Annu. Rev. Cell. Dev. Biol. **11:**471–495.
33. **Jin, Q. W., J. Fuchs, and J. Loidl.** 2000. Centromere clustering is a major determinant of yeast interphase nuclear organization. J. Cell Sci. **113:**1903–1912.
34. **Keith, K. C., and M. Fitzgerald-Hayes.** 2000. *CSE4* genetically interacts with the *Saccharomyces cerevisiae* centromere DNA elements CDE I and CDE II but not CDE III: implications for the path of the centromere DNA around a Cse4p variant nucleosome. Genetics **156:**973–981.
35. **Kingston, R. E., and G. J. Narlikar.** 1999. ATP-dependent remodeling and acetylation as regulators of chromatin fluidity. Genes Dev. **13:**2339–2352.
36. **Koshland, D., and P. Hieter.** 1987. Visual assay for chromosome ploidy. Methods Enzymol. **155:**351–372.
37. **Laurent, B. C., X. Yang, and M. Carlson.** 1992. An essential *Saccharomyces cerevisiae* gene homologous to *SNF2* encodes a helicase-related protein in a new family. Mol. Cell. Biol. **12:**1893–1902.
38. **Li, L., S. J. Elledge, C. A. Peterson, E. S. Bales, and R. J. Legerski.** 1994. Specific association between the human DNA repair proteins XPA and ERCC1. Proc. Natl. Acad. Sci. USA **91:**5012–5016.
39. **Lorch, Y., M. Zhang, and R. Kornberg.** 2001. RSC unravels the nucleosome. Mol. Cell **7:**89–95.
40. **Mehta, S., X. M. Yang, C. S. Chan, M. J. Dobson, M. Jayaram, and S. Velmurugan.** 2002. The 2 micron plasmid purloins the yeast cohesin complex: a mechanism for coupling plasmid partitioning and chromosome segregation? J. Cell Biol. **158:**625–637.
41. **Meluh, P. B., and D. Koshland.** 1997. Budding yeast centromere composition and assembly as revealed by in vivo cross-linking. Genes Dev. **11:**3401–3412.
42. **Meluh, P. B., and D. Koshland.** 1995. Evidence that the MIF2 gene of *Saccharomyces cerevisiae* encodes a centromere protein with homology to the mammalian centromere protein CENP-C. Mol. Biol. Cell **6:**793–807.
43. **Meluh, P. B., P. Yang, L. Glowczewski, D. Koshland, and M. M. Smith.** 1998. Cse4p is a component of the core centromere of Saccharomyces cerevisiae. Cell **94:**607–613.
44. **Michaelis, C., R. Ciosk, and K. Nasmyth.** 1997. Cohesins: chromosomal proteins that prevent premature separation of sister chromatids. Cell **91:**35–45.
45. **Moreira, J. M., and S. Holmberg.** 1999. Transcriptional repression of the yeast CHA1 gene requires the chromatin-remodeling complex RSC. EMBO J. **18:**2836–2844.
46. **Nasmyth, K.** 2002. Segregating sister genomes: the molecular biology of chromosome separation. Science **297:**559–565.
47. **Ng, H. H., F. Robert, R. A. Young, and K. Struhl.** 2002. Genome-wide location and regulated recruitment of the RSC nucleosome-remodeling complex. Genes Dev. **16:**806–819.
48. **Ortiz, J., O. Stemmann, S. Rank, and J. Lechner.** 1999. A putative protein complex consisting of Ctf19, Mcm21, and Okp1 represents a missing link in the budding yeast kinetochore. Genes Dev. **13:**1140–1155.
49. **Pearson, C. G., P. S. Maddox, E. D. Salmon, and K. Bloom.** 2001. Budding yeast chromosome structure and dynamics during mitosis. J. Cell Biol. **152:**1255–1266.
50. **Pidoux, A. L., and R. C. Allshire.** 2000. Centromeres: getting a grip of chromosomes. Curr. Opin. Cell Biol. **12:**308–319.
51. **Pinto, I., and F. Winston.** 2000. Histone H2A is required for normal centromere function in *Saccharomyces cerevisiae*. EMBO J. **19:**1598–1612.
52. **Recht, J., and M. A. Osley.** 1999. Mutations in both the structured domain and N-terminus of histone H2B bypass the requirement for Swi/Snf in yeast. EMBO J. **18:**101–113.
53. **Rose, M. D., F. Winston, and P. Hieter.** 1990. Methods in yeast genetics: a laboratory course manual. Cold Spring Harbor Press, Cold Spring Harbor, N.Y.
54. **Saunders, M., M. Fitzgerald-Hayes, and K. Bloom.** 1988. Chromatin structure of altered yeast centromeres. Proc. Natl. Acad. Sci. USA **85:**175–179.
55. **Saunders, M. J., E. Yeh, M. Grunstein, and K. Bloom.** 1990. Nucleosome depletion alters the chromatin structure of *Saccharomyces cerevisiae* centromeres. Mol. Cell. Biol. **10:**5721–5727.
56. **Schulman, I., and K. S. Bloom.** 1991. Centromeres: an integrated protein/DNA complex required for chromosome movement. Annu. Rev. Cell Biol. **7:**311–336.
57. **Sengupta, S. M., M. VanKanegan, J. Persinger, C. Logie, B. R. Cairns, C. L. Peterson, and B. Bartholomew.** 2001. The interactions of yeast SWI/SNF and RSC with the nucleosome before and after chromatin remodeling. J. Biol. Chem. **276:**12636–12644.
58. **Sharp, J. A., A. A. Franco, M. A. Osley, and P. D. Kaufman.** 2002. Chromatin assembly factor I and Hir proteins contribute to building functional kinetochores in *S. cerevisiae*. Genes Dev. **16:**85–100.
59. **Shen, X., G. Mizuguchi, A. Hamiche, and C. Wu.** 2000. A chromatin remodelling complex involved in transcription and DNA processing. Nature **406:**541–544.
60. **Sikorski, R. S., and J. D. Boeke.** 1991. *In vitro* mutagenesis and plasmid shuffling: from cloned gene to mutant yeast. Methods Enzymol. **199:**302–318.
61. **Sikorski, R. S., and P. Hieter.** 1989. A system of shuttle vectors and yeast host strains designed for efficient manipulation of DNA in *Saccharomyces cerevisiae*. Genetics **122:**19–27.
62. **Skibbens, R. V., and P. Hieter.** 1998. Kinetochores and the checkpoint mechanism that monitors for defects in the chromosome segregation machinery. Annu. Rev. Genet. **32:**307–337.
63. **Smith, M. M.** 2002. Centromeres and variant histones: what, where, when, and why? Curr. Opin. Cell Biol. **14:**279–285.
64. **Smith, M. M., P. Yang, M. S. Santisteban, P. W. Boone, A. T. Goldstein, and P. C. Megee.** 1996. A novel histone H4 mutant defective in nuclear division and mitotic chromosome transmission. Mol. Cell. Biol. **16:**1017–1026.
65. **Sorger, P. K., K. F. Doheny, P. Hieter, K. M. Kopski, T. C. Huffaker, and A. A. Hyman.** 1995. Two genes required for the binding of an essential *Saccharomyces cerevisiae* kinetochore complex to DNA. Proc. Natl. Acad. Sci. USA **92:**12026–12030.
66. **Strahl, B. D., and C. D. Allis.** 2000. The language of covalent histone modifications. Nature **403:**41–45.
67. **Sudarsanam, P., and F. Winston.** 2001. The Swi/Snf family: nucleosome-remodeling complexes and transcriptional control. Trends Genet. **16:**345–351.
68. **Sullivan, K. F.** 2001. A solid foundation: functional specialization of centromeric chromatin. Curr. Opin. Genet. Dev. **11:**182–188.
69. **Tanaka, T., M. P. Cosma, K. Wirth, and K. Nasmyth.** 1999. Identification of cohesin association sites at centromeres and along chromosome arms. Cell **98:**847–858.
70. **Tanaka, T. U.** 2002. Bi-orienting chromosomes on the mitotic spindle. Curr. Opin. Cell Biol. **14:**365–371.
71. **Treich, I., and M. Carlson.** 1997. Interaction of a Swi3 homolog with Sth1 provides evidence for a Swi/Snf-related complex with an essential function in *Saccharomyces cerevisiae*. Mol. Cell. Biol. **17:**1768–1775.
72. **Treich, I., L. Ho, and M. Carlson.** 1998. Direct interaction between Rsc6 and Rsc8/Swh3, two proteins that are conserved in SWI/SNF-related complexes. Nucleic Acids Res. **26:**3739–3745.
73. **Tsuchiya, E., T. Hosotani, and T. Miyakawa.** 1998. A mutation in *NPS1*/*STH1*, an essential gene encoding a component of a novel chromatin-remodeling complex RSC, alters the chromatin structure of *Saccharomyces cerevisiae* centromeres. Nucleic Acids Res. **26:**3286–3292.
74. **Tsuchiya, E., M. Uno, A. Kiguchi, K. Masuoka, Y. Kanemori, S. Okabe, and T. Mikayawa.** 1992. The *Saccharomyces cerevisiae NPS1* gene, a novel *CDC* gene which encodes a 160 kDa nuclear protein involved in G_2 phase control. EMBO J. **11:**4017–4026.
75. **Van Hooser, A. A., Ouspenski, I. I., H. C. Gregson, D. A. Starr, T. J. Yen, M. L. Goldberg, K. Yokomori, W. C. Earnshaw, K. F. Sullivan, and B. R. Brinkley.** 2001. Specification of kinetochore-forming chromatin by the histone H3 variant CENP-A. J. Cell Sci. **114:**3529–3542.
76. **Vignali, M., A. H. Hassan, K. E. Neely, and J. L. Workman.** 2000. ATP-dependent chromatin-remodeling complexes. Mol. Cell. Biol. **20:**1899–1910.
77. **Wong, M. C., S. R. Scott-Drew, M. J. Hayes, P. J. Howard, and J. A. Murray.** 2002. RSC2, encoding a component of the RSC nucleosome remodeling complex, is essential for 2μm plasmid maintenance in *Saccharomyces cerevisiae*. Mol. Cell. Biol. **22:**4218–4229.
78. **Xue, Y., J. C. Canman, C. S. Lee, Z. Nie, D. Yang, G. T. Moreno, M. K. Young, E. D. Salmon, and W. Wang.** 2000. The human SWI/SNF-B chromatin-remodeling complex is related to yeast *rsc* and localizes at kinetochores of mitotic chromosomes. Proc. Natl. Acad. Sci. USA **97:**13015–13020.